Supplemental Materials

Molecular Biology of the Cell

Arndt et al.

SUPPLEMENTAL MATERIALS FOR:

NAADP and the Two Pore channel Protein TPC1 participate in the Acrosome Reaction in Mammalian Spermatozoa

Lilli Arndt, Jan Castonguay, Elisabeth Arlt, Dorke Meyer, Sami Hassan, Heike Borth, Susanna Zierler, Gunther Wennemuth, Andreas Breit, Martin Biel, Christian Wahl-Schott, Thomas Gudermann, Norbert Klugbauer, Ingrid Boekhoff

Supplemental Information: Material

General reagents and antibodies

Sources of antibodies and chemicals are the following: A rabbit polyclonal anti-inositol 1,4,5-triphosphate receptor (IP_3R) IgG raised to amino acids 2731–2749 of the rat type-I IP_3-R, which was recommended for the detection of all three IP_3R isoforms of mouse, rat and human origin as well as its immunogenic peptide were obtained from Synaptic Systems ([117002, 117-0P], Göttingen, Germany); the polyclonal anti-caveolin-1 IgG (sc-894) generated against the N-terminus of caveolin-1 of human origin which was also recommended for the detection of caveolin-1 of mouse and rat was obtained from Santa Cruz Biotechnology (Heidelberg, Germany). Applied secondary antibodies were the following: A fluorescein isothiocyanate (FITC)-conjugated goat anti-rabbit IgG was purchased from Sigma-Aldrich (Deisenhofen, Germany), a horseradish peroxidase (HRP)-conjugated goat anti-rabbit IgG was obtained from Bio-Rad (Munich, Germany), HRP-conjugated sheep anti-mouse IgG was provided by GE Healthcare (Buckinghamshire, UK), the used anti-goat HRP-coupled donkey IgG was supplied by Santa Cruz Biotechnology (Heidelberg, Germany), the Avidin-Biotin complex (ABC)-peroxidase kit (Vectastain ABC elite kit) used for immunohistochemical experiments was provided by Biozol (Eching, Germany). Tetramethyl rhodamine isothiocyanate (TRITC)-conjugated *peanut agglutinin* (PNA) as well as propidium jodide, the pore-forming bacterial toxin streptolysin O (SLO) (Johnson et al., 1999), the calcium ionophor A23187 (Liu and Baker, 1990), the ryanodine receptor (RyR) antagonist ruthenium red (RR) (Ozawa, 2010), the IP_3-R inhibitor 2-aminoethyldiphenyl borate (2-APB) (Bootman et al., 2002), nicotinic acid adenine dinucleotide phosphate sodium salt (NAADP) and Triton X-100 were obtained from Sigma Aldrich (Deisenhofen, Germany); the vascular-type proton-translocating ATPase inhibitor Bafilomycin (Bowman et al., 1988) was from Santa Cruz Biotechnology (Heidelberg, Germany), the nuclear staining dye TO-PRO-3 was purchased by Invitrogen (Karlsruhe, Germany), the detergent Nonidet-P40 was obtained from Calbiochem-Novabiochem (Bad Soden, Germany), paraformaldehyde was obtained from Sciences Services (Munich, Germany); nicotinamide adenine dinucleotide phosphate disodium salt (NADP) was obtained from Merck (Darmstadt, Germany). The red-fluorescent dye LysoTracker Red DND-99 for staining of acidic cellular organelles (Moreno et al., 2010) was obtained from Invitrogen (Darmstadt, Germany), Fluo-8-AM was obtained from AAT Bioquest (Sunnyvale, CA, USA); the NAADP antagonist, *trans*-Ned-19 (Naylor et al., 2009) was provided by Enzo Life Sciences GmbH (Lörrach, Germany). For protease inhibition a protease inhibitor cocktail III (Calbiochem-Novabiochem, Bad Soden, Germany) was applied. Primers were ordered from Metabion (Planegg-Martinsried, Germany). Unless specified otherwise, standard laboratory reagents were either purchased from Sigma-Aldrich (Deisenhofen, Germany) or Carl Roth (Karlsruhe, Germany).

Supporting Information: Methods

Reverse transcriptase-polymerase chain reaction (RT-PCR) and PCR for genotyping

Reverse transcriptase-PCR analyses were performed as described recently (Meyer et al., 2012). Briefly, total RNA, isolated from adult mouse kidney and testis tissue (Nucleospin, Machery-Nagel, Düren, Germany) was reverse-transcribed using the Supercript III reverse transcriptase and oligo-dT primers according to the manufacturer's recommendations (Invitrogen, Karlsruhe, Germany). For the amplification of subtype-specific TPC-derived fragments, reverse-transcribed cDNA from kidney and testis tissue was initially examined for contamination with genomic DNA using exon spanning primer pairs of beta-actin (accession number NM007393), 5´-GGCTACAGCTTCACCACCAC-3` (forward) and 5`-GAGTACTTGGCGTCAGGAGG-3` (reverse) (Ziegler et al., 1992). The oligonucleotide primers for TPC1 and TPC2 were based on published mRNA sequences of mice: TPC1 (accession number: BC058951), 5´-CACAACTGGGAGATGAATTATCA-3 (forward) and 5´-TTGAAGGTGTCGAACACCA CG-3´ (reverse) [accepted PCR-amplification product: 778 bp]; TPC2: (accession number: NM_14620 6), 5´-GACAACACCTCAGCTGTATGTG-3´ (forward) and 5´-TGCCGACTAATGGTCTGCCAA-3´ (reverse) [accepted PCR-amplification product: 605 bp]. Amplification of the TPC sequences were performed in a volume of 25 µl containing 2.5 µl 10 x PCR buffer), 0.8 mMdNTPs, 0.125 µl Taq DNA polymerase (both Fermentas, St. Leon-Rot, Germany), 4 pmol of each primer and 1 µl of quality-checked cDNA. Optimized PCR conditions consisted of 30 (TPC1, TPC2) or 35 (actin) cycles at 94 °C for 1 min, followed by annealing for 1 min and elongation at 72 °C for 1 min. The PCR program

finished with a final annealing period at 72 °C for 7 min. Following PCR reactions, aliquots of amplicons (10 µl) were analyzed by electrophoresis on agarose gels containing ethidium bromide. Sizes of amplification products were compared with a 100 bp molecular weight marker (Fermentas, St. Leon-Rot, Germany); identity of the amplicons was verified by sequencing (MWG Biotech, Ebersberg, Germany).
For mouse PCR genotyping tail DNA extraction was performed as described recently (Meyer et al., 2012). Genotyping primers were the following: TPC1: 5`-TCA GCT GCC TGT GAG CCA GAG-3´ (forward), 5`-GGA GCT CAC CTG GTT GTG CCA TA-3 (reverse). The expected DNA product size for the wild-type was 390 bp. TPC1 knockout: 5´-TCA GCT GCC TGT GAG CCA GAG-3´ (forward) 5´-CCA TGC CTT TGA TCC CAA CAA-3´ [reverse]. The expected size of amplification product was 290 bp. PCR was performed with the following conditions: 2.5 µl 10 x PCR-buffer, 0.8 mM dNTPs, 0.125 µl Taq DNA polymerase, 4 pmol of each primer and 1 µl of isolated genomic tail DNA were mixed in a total amplification volume of 25 µl. PCR reactions were preheated at 94 °C for 5 min; PCR conditions consisted of 30 cycles denaturation at 94 °C for 1 min, annealing at 61 °C for 1 min and elongation at 72 °C for 1 min followed by an extra extension step of 10 min at 72 °C.

Sperm preparation
Sperm from adult mice and rats from sexually mature animals were isolated as described recently (Ackermann et al., 2009). Briefly, caudal epididymis were excised, freed of fat and transferred to small dishes containing pre-warmed (37 °C) HS buffer (30 mM HEPES, 135 mM NaCl, 5 mM KCl, 2 mM $CaCl_2$, 1 mM $MgSO_4$, 10 mM glucose, 10 mM lactic acid, and 1 mM pyruvic acid, pH 7.4). To obtain capacitated spermatozoa for functional assays, caudae epididymides were transferred to HS buffer supplemented with 0.5 % BSA and 15 mM $NaHCO_3$ (capacitation buffer) and incised several times with a scalpel to allow motile sperm to exude into the medium. After a “swim out“ period of 90 min at 37 °C and 5 % CO_2, dispersed sperm suspension was collected by centrifugation (5 min, 400 g, RT), and either resuspended in modified Krebs Ringer bicarbonate buffer (KRB) (5.6 mM glucose, 0.55 mM sodium-pyruvate, 25 mM Na_2HCO_3, 53 mM sodium-lactate, 99.6 mM NaCl, 4.8 mM KCl, 1.2 mM K_2HPO_4, 1.2 mM $MgSO_4$; pH 7.4) and immediately used for functional acrosome reaction assays, or washed twice with PBS and used to isolate membrane for Western blot analyses. Western blot experiments performed with membrane fractions of ejaculated human semen samples from young healthy donors where carried out as described recently (Meyer et al., 2012).

Single Cell Calcium Imaging
To determine changes in intracellular calcium concentrations in the sperm head, mouse spermatozoa were isolated as described above and incubated in HS buffer supplemented with 0.5 % BSA and 15 mM $NaHCO_3$ (capacitation buffer) for 60 min. Subsequently, cells were centrifuged at 400 g for 5 min at RT and washed twice with HS/$NaHCO_3$. Cells were resuspended in 1 ml HS/$NaHCO_3$ containing Pluronic (0.003 % final concentration) and 10 µM Fluo8-AM and then incubated for 30 min at RT. After two washes with HS/$NaHCO_3$ and centrifugation at 400 g for 5 min, cells were resuspended in HS/$NaHCO_3$ and incubated for 30 min at RT to allow de-esterification of the fluorescence dye before starting the measurement. Sperm cells were then adhered to coverslips coated with laminin (50 µg/ml in PBS) and poly-L-ornithine (0.01 % in H_2O) for 1 min, and subsequently washed twice with HS/$NaHCO_3$ to eliminate non-adherent cells.
Fluorimetric determination of changes in light intensity (excitation 485 nm/emission 520 nm) in the sperm head was monitored over time using a Polychrome V monochromator (Till-Photonics, Gräfelfing, Germany) and an Andor charge-coupled device camera coupled to an inverted microscope (IX71, Olympus, Hamburg, Germany). For a typical time course experiment, basal Ca^{2+} was initially determined, taking 15 pictures with a 2 sec interval. Thereafter, cells were either treated with buffer used as a negative control to follow application artifacts, or HS/$NaHCO_3$ containing different stimuli. Changes in fluorescence intensity were determined for about 240 sec before cell viability was verified adding 5 µM of the calcium ionophore ionomycin. Only cells showing a robust response to ionomycin were included into the calculations. Changes in fluorescence for every time point of the experiment were determined calculating the quotient of fluorescence signals registered upon stimuli application to basal fluorescence intensity (100 %).

Membrane preparation, isolation of Triton X-100 insoluble membrane fractions and Western-Blot analyses
Membrane enriched and cytosolic fractions of mouse kidney, testes and intact epididymis not depleted from sperm were prepared as described recently (Ackermann et al., 2008). Briefly, freshly dissected tissue was transferred to ice-cold hypotonic TME-buffer (10 mM Tris, 2 mM $MgCl_2$, 3 mM EGTA, protease inhibitor cocktail, pH 7.4) and lysed by homogenization and sonication (30 sec, 48C, Model 7100, MSE, London, UK). To separate cell nuclei and intact organelles, homogenate was

centrifuged two times for 10 min at 2,500 g and 4 °C (Biofuge Stratus-Heraeus). The pooled supernatants (S_1) were subsequently centrifuged for 1 h at 100,000 g and 4°C in a Ti50 fixed angle rotor (Beckman Coulter), and the resulting supernatants containing cytosolic proteins (S_2) as well as the pellet presenting the membrane fraction (P_2) were stored in TME-diluted aliquots (2 mg/ml) at -70 °C. Protein concentrations were measured by the Bradford method (Bradford, 1976). For fractionation of epididymal rat and mouse sperm, cells were treated in the same way than described for the different tissues, except that TME-buffer was supplemented with 0.25 % NP-40.

Glycolipid-enriched raft membrane subdomains were isolated from capacitated rat sperm as described previously (Travis *et al.*, 2001; Ackermann *et al.*, 2008). Briefly, motile epididymal rat spermatozoa were transferred to 100 mM Tris-HCl, pH 8.0, 300 mM sucrose, pH 7.4, Complete proteinase inhibitor cocktail (Roche), lysed by homogenization and sonication (2 min, 4 °C) and stored at -80°C. Detergent-resistant membranes (DRMs) of thawed spermatozoa were subsequently enriched by fractional centrifugation. To first separate cell nuclei and intact organelles from soluble and membrane proteins, homogenized germ cells were centrifuged for 10 min at 10,000 g. The pooled supernatants containing the DRMs were subsequently centrifuged for 2 h at 100,000 g (Ti50 rotor, Beckman Coulter), and the resulting pellet (P_{100}) extracted for 30 min at 4 °C with ice-cold PBS supplemented with 1.5 % Triton X-100. After an additional centrifugation step for 2 h at 50,000 g, Triton X-100 soluble fractions (S_{Tx}) were separated from the detergent insoluble membrane fractions in the pellet (P_{Tx}). Protein concentration in the obtained three fractions was determined according to Bradford (Bradford, 1976), using corresponding Triton X-100 dilutions as blank samples. To determine TPC1 positive fractions equivalent amounts of the total membrane starting material (P100), as well as the detergent insoluble (P_Tx) and soluble fractions (S_Tx) were separated by SDS–PAGE and analyzed by Western blot analysis as described previously (Ackermann et al., 2008). Therefore, protein of each fraction diluted with 5 x sample buffer (625 mM Tris/HCl, pH 6.8, 50 % glycerol, 5 % SDS, 7.5 mM dithiothreitol, 0.05 % bromphenol blue), was boiled for 5 min, separated by SDS-PAGE, transferred to nitrocellulose using a semidry blotting system and stained with Ponceau S to ensure equal protein loading of each reaction. After blocking non-specific binding sites on the nitrocellulose sheets with 5 % powdered non-fat milk in 10 mM Tris/HCl, pH 8.0, 150 mM NaCl and 0.05 % Tween 20 (TBST), blots were incubated overnight at 4 °C with specific primary antibodies diluted in TBST supplemented with 3 % powdered milk. After three washing steps with TBST, a horseradish-peroxidase-conjugated secondary antibody, diluted in TBST containing 3 % non-fat milk powder, respectively, was applied for 1 h at RT. Excess antibody was then removed by three washing steps with TBST, and subsequently the ECL-system (100 mM Tris-HCl, 2.5 mM luminol, 0.4 mM p-coumaric acid; pH 8.5, and 100 mM Tris-HCl, 18 µM H_2O_2; pH 8.5) (1:1, v/v) was used to visualize bound antibodies. Chemoluminescence was detected using an automated chemiluminescence system (Peqlab, Erlangen, Germany). For proteins which specifically partition into the DRM fraction, the raft marker caveolin-1 (Anderson, 1998) was used. To ensure equal protein loading on SDS PAGEs analyzing tissue of wild-type and TPC1 null animals, fractionated protein of the same tissue preparation was separated on 12 % SDS PAGES and also probed with the anti-caveolin-1 antibody.

Supporting Information: References

Ackermann, F., Zitranski, N., Borth, H., Buech, T., Gudermann, T., and Boekhoff, I. (2009). CaMKIIalpha interacts with multi-PDZ domain protein MUPP1 in spermatozoa and prevents spontaneous acrosomal exocytosis. Journal of cell science *122*, 4547-4557.

Ackermann, F., Zitranski, N., Heydecke, D., Wilhelm, B., Gudermann, T., and Boekhoff, I. (2008). The Multi-PDZ domain protein MUPP1 as a lipid raft-associated scaffolding protein controlling the acrosome reaction in mammalian spermatozoa. Journal of cellular physiology *214*, 757-768.

Anderson, R.G. (1998). The caveolae membrane system. Annu Rev Biochem *67*, 199-225.

Bootman, M.D., Collins, T.J., Mackenzie, L., Roderick, H.L., Berridge, M.J., and Peppiatt, C.M. (2002). 2-aminoethoxydiphenyl borate (2-APB) is a reliable blocker of store-operated Ca2+ entry but an inconsistent inhibitor of InsP3-induced Ca2+ release. Faseb J *16*, 1145-1150.

Bowman, E.J., Siebers, A., and Altendorf, K. (1988). Bafilomycins: a class of inhibitors of membrane ATPases from microorganisms, animal cells, and plant cells. Proceedings of the National Academy of Sciences of the United States of America *85*, 7972-7976.

Bradford, M.M. (1976). A rapid and sensitive method for the quantitation of microgram quantities of protein utilizing the principle of protein-dye binding. Analytical biochemistry *72*, 248-254.

Johnson, L.R., Moss, S.B., and Gerton, G.L. (1999). Maintenance of motility in mouse sperm permeabilized with streptolysin O. Biology of reproduction *60*, 683-690.

Liu, D.Y., and Baker, H.W. (1990). Inducing the human acrosome reaction with a calcium ionophore A23187 decreases sperm-zona pellucida binding with oocytes that failed to fertilize in vitro. Journal of reproduction and fertility *89*, 127-134.

Meyer, D., Voigt, A., Widmayer, P., Borth, H., Huebner, S., Breit, A., Marschall, S., de Angelis, M.H., Boehm, U., Meyerhof, W., Gudermann, T., and Boekhoff, I. (2012). Expression of tas1 taste receptors in Mammalian spermatozoa: functional role of tas1r1 in regulating Basal ca and cAMP concentrations in spermatozoa. PloS one *7*, e32354.

Moreno, A., SantoDomingo, J., Fonteriz, R.I., Lobaton, C.D., Montero, M., and Alvarez, J. (2010). A confocal study on the visualization of chromaffin cell secretory vesicles with fluorescent targeted probes and acidic dyes. Journal of structural biology *172*, 261-269.

Naylor, E., Arredouani, A., Vasudevan, S.R., Lewis, A.M., Parkesh, R., Mizote, A., Rosen, D., Thomas, J.M., Izumi, M., Ganesan, A., Galione, A., and Churchill, G.C. (2009). Identification of a chemical probe for NAADP by virtual screening. Nature chemical biology *5*, 220-226.

Ozawa, T. (2010). Modulation of ryanodine receptor Ca2+ channels (Review). Molecular medicine reports *3*, 199-204.

Travis, A.J., Merdiushev, T., Vargas, L.A., Jones, B.H., Purdon, M.A., Nipper, R.W., Galatioto, J., Moss, S.B., Hunnicutt, G.R., and Kopf, G.S. (2001). Expression and localization of caveolin-1, and the presence of membrane rafts, in mouse and Guinea pig spermatozoa. Developmental biology *240*, 599-610.

Ziegler, B.L., Lamping, C., Thoma, S., and Thomas, C.A. (1992). Single-cell cDNA-PCR: removal of contaminating genomic DNA from total RNA using immobilized DNase I. Biotechniques *13*, 726-729.

Table 1
Effect of NAADP on acrosome reaction in uncapacitated spermatozoa.

conditions	acrosome reaction [%]
30 min	10.03 ± 2.61
60 min	10.65 ± 1.40
Ca^{2+}	30.12 ± 1.21 (**)
Ca^{2+} + A23187	56.30 ± 6.07 (**)
50 nM NAADP	11.81 ± 1.41
1 µM NAADP	12.00 ± 1.95
50 µM NAADP	13.57 ± 2.15

To assess whether NAADP in uncapacitated spermatozoa is able to drive acrosome reaction, permeabilized sperm, isolated in HS buffer without $NaHCO_3$ and BSA, were incubated for 30 min at 37 °C in KRB/SLO buffer. Samples were stimulated with one of the three NAADP concentrations which in capacitated sperm were observed to induce maximal acrosomal exocytosis rates (s. Figure 5A and B). To verify that sperm of each preparation are indeed able to undergo acrosomal secretion, two positive controls were included in which spermatozoa were incubated for 30 min in KRB-buffer supplemented with 10 mM $CaCl_2$ or $CaCl_2$ together with 10 µM of the Ca^{2+} ionophor A23187, respectively. Note that none of the three NAADP doses in uncapacitated sperm increased the proportion of acrosome reacted sperm, whereas a stimulation with Ca^{2+} and Ca^{2+} together with A23187 significantly elevated acrosome reaction rates compared to samples incubated in control buffer. Data are presented as absolute percentage of acrosome-reacted sperm. Averages of 4 independent experiments with different mouse sperm preparations are shown. Statistical significance ([*: $p < 0.05$], [**: $p < 0.01$], [***: $p < 0.001$]) was considered if data were different from rates of spontaneous loss of the acrosomal vesicle [60 min].

Table 2
Effect of NAADP on acrosome reaction in non-permeabilized spermatozoa

conditions	acrosome reaction [%]
90 min	17.46 ± 1.71
120 min	16.79 ± 1.71
Ca^{2+}	32.67 ± 2.96 (**)
Ca^{2+} + A23187	73.47 ± 1.35 (**)
50 nM NAADP	17.18 ± 0.69
1 µM NAADP	18.50 ± 2.58
50 µM NAADP	18.57 ± 3.92

Capacitated but non-permeabilized spermatozoa were incubated for 30 min at 37 °C in KRB buffer or KRB buffer supplemented with NAADP concentrations, which in the performed dose-response relationships studies were observed to elicit maximal secretion rates (Figure 5A and B). Note that an increase in Ca^{2+}, either upon application of 10 mM $CaCl_2$ or by the addition of $CaCl_2$ together with the Ca^{2+} ionophore A23187 (10 µM) led to a significant increase in the incidence of exocytosis, whereas none of the added NAADP concentrations elevated secretion rates. Data presented as percentage of acrosome reacted-sperm are the mean values ± SEM of 4 independent experiments of different mouse sperm preparations. Obtained data were subjected to a Student's t-test for determination of significant differences. Statistical significance ([*: $p < 0.05$], [**: $p < 0.01$], [***: $p < 0.001$]) was considered if data were different from rates of spontaneous loss of the acrosomal vesicle [120 min].

Supporting Information: Legends

Figure S1. Detection of TPC-transcripts from cDNA of murine kidney and testicular tissue using RT-PCR.
Primer sets specific for the murine TPCN1 and TPCN2 yielded in amplification products with the predicted size ([*TPC1*], 778 bp; ([*TPC2*], 605 bp) in cDNA derived from kidney ([*kidney*]*)* as well as from testicular tissue ([*testis*]). Integrity of cDNA was verified using a primer pair against the housekeeping gene *β-actin* ([*β-actin*]; 425 bp). Negative controls represent samples in which water was used instead of cDNA ([H_2O]). The sizes of amplification products were compared with a 100-bp molecular weight marker ([*bp*]) shown in the left margin of each panel.

Figure S2. Validation of a TPC1 specific antibody using kidney tissue of wild-type and TPC1 knockout mice.
Equal amounts of whole kidney tissue ([*S1*]) as well as cytosolic ([*S2*]) and membrane fractions ([*P2*]) of wild-type ([+/+]) and TPC1 knockout mice ([-/-]) were subjected to Western blot analysis using a subtype-specific antibody (TPC1NK). Equal amounts of protein of the same tissue preparations were validated with an antibody recognizing the raft marker protein caveolin-1 [*Cav-1*]. The anti-TPC1NK antibody labeled a band with the predicted size of TPC1 of about 94 kDa in kidney tissue of wild-type animals (left part of the top panel, [*TPC1 [+/+]*]). A comparison of the relative band intensities in cytosolic and membrane kidney fractions revealed that the TPC1 channel protein is associated with kidney membrane proteins. Experiments were repeated with at least three independent tissue preparations. The positions of the molecular weight standards (in kDa) are indicated on the left of each panel. The arrow indicates the respective expected protein weight.

Figure S3. Effect of TPC1 deficiency on morphology of reproductive tissue and spermatozoa.
[**A**] Morphological analysis of reproductive organs of TPC1 null male mice. Representative photomicrographs of Hematoxylin-Eosin stained sections of testis and epididymis of wild-type [+/+] and TPC1 knockout males [-/-] were examined for abnormalities during spermatogenesis. Note that microscopic comparison of seminiferous tubules (dotted line, [*st*]) of testis from TPC1 null mutants versus wild-type males does not reveal obvious differences. Mice lacking TPC1 show no apparent differences in the number or size of seminiferous tubules, or changes in the ordered concentric layers of different developing germ cell populations. The same was true analyzing coronal sections of the caput and caudal epididymis. Lumen of epididymal ducts (dotted line, [*ed*]) of the caput and cauda regions of the two examined male genotypes contain densely packed mature spermatozoa (arrowhead, [*s*]) with no obvious difference. The presented micrographs are representatives of histological analyses of 3 adult TPC1 knockout and wild-type littermates. The schematic drawing shows a sagittal section through testes and the caput and cauda region of the epididymis. *ed*, epididymal duct; *s*, spermatozoa; *st*, seminiferous tubule.
[**B**] Morphology of TPC1 null sperm. Caudal epididymal sperm from wild-type animals [+/+] and TPC1-deficient mice [-/-] were both fixed and subsequently transferred to Coomassie brilliant blue staining (left panel pair, [*CB*]), or incubated with FITC-conjugated PNA lectine (middle panel pair, ([*PNA*]). To additionally assess whether NAADP binding sites were altered in sperm upon TPCN1 gene deletion, living epididymal sperm of wild-type and TPC1 deficient sperm were incubated with 100 µM of the NAADP antagonist *trans*-Ned-19 (right panel pair, ([*Ned19*]), and subsequently subjected to fluorescence microscopy. Photomicrographs illustrate that TPC1 null sperm possess a normally formed flagellum and do not exhibit obvious structural defects in the acrosome compared to wild-type sperm. Moreover, it was found that NAADP binding sites visualized by the fluorescence dye *trans*-Ned-19 were obviously not changed upon TPC1 deletion, concerning their localization and signal intensity. Presented fluorescence micrographs are representative images of age-matched TPC1 knockout and wild-type males. Identical illumination intensity and camera settings were applied.

Figure S4. Determination of the effect of the selective NAADP antagonist *trans*-Ned-19 on acrosome reaction.
[**A**] Effect of 100 µM *trans*-Ned-19 on NAADP-induced acrosome reaction. To assess the impact of high *trans*-Ned-19 concentrations on NAADP-induced acrosome reaction, capacitated and permeabilized sperm were stimulated either with NAADP doses found to elicit maximal acrosomal secretion rates (50 nM, 1 µM, 50 µM) or NAADP together with 100 µM *trans*-Ned-19. Note that high *trans*-Ned-19 doses did not antagonize responsiveness induced by the three NAADP concentrations but, albeit not significant, slightly increased acrosomal secretion rates. Results are presented as mean values ± SEM, normalized by subtracting the number of reacted spermatozoa incubated in KRB/SLO buffer only (negative control) and expressed as percentage of maximal acrosome reaction rates induced upon application of 10 mM $CaCl_2$ (n = 6). Statistical significance was calculated

comparing samples stimulated with one of the three NAADP doses alone with probes incubated with NAADP together with *trans*-Ned-19. Statistical analysis was done using a paired Student's t-test (n.s.: not significant).
[**B**] Effect of *trans*-Ned-19 on intracellular calcium concentrations in spermatozoa. To determine the effect of *trans*-Ned-19 on intracellular Ca^{2+} concentrations, capacitated sperm (C57BL/6) were loaded with the calcium fluorescent dye Fluo8-AM (10 µM). Subsequently fluorescence intensity was determined at the excitation wavelength of Fluo8-AM (485 nm) using an YFP filter and a microscope based imaging system. After taking a baseline to determine the fluorescence in the head region of resting sperm, different concentrations of *trans*-Ned-19 (50 µM, 100 µM) or control buffer were added, and fluorescence emission was determined for an additional period of 200 sec. Finally cell viability was confirmed by adding 5 µM of the cation ionophore ionomycin. Note that the addition of buffer or 50 µM *trans*-Ned-19 barely evoked any changes in Fluo8 fluorescence, whereas 100 µM *trans*-Ned-19 induced a clear, transient increase in intracellular Ca^{2+} concentration, $[Ca^{2+}]_i$. Fluorescence intensity, measured every 2 sec, was calculated as ratio to basal Fluo8 emission (F_0, 100%). Presented data show mean values ± SEM of 3 different sperm preparations (total number of analzyed sperm: 14 – 27 cells/animal).

Figure S5. Functional relation between NAADP-triggered acrosome reaction and Ca^{2+} channels of intracellular organelles.
[**A**] Effects of IP_3 receptor antagonist, 2-APB, and ryanodine receptor antagonist, ruthenium red, on spontaneous acrosome reaction. To determine the effect of IP_3R and RyR inhibition on spontaneous acrosomal secretion, capacitated and permeabilized sperm of C57BL/6 mice were either incubated for 45 min in KRB/SLO buffer [*control*], or pretreated with the IP_3-R sensitive Ca^{2+} channel inhibitor, 2-APB ([*2-APB*], 10 µM) or the RyR antagonist, ruthenium red ([*RR*], 10 µM). Note that neither RR nor 2-ABP changed basal acrosomal secretion rates. The results of acrosome reacted sperm are presented as mean values of 6 – 10 independent experiments ± SEM and expressed as absolute percentage of induced acrosome reacted sperm.
[**B** and **C**] Effects of ryanodine receptor antagonist, ruthenium red, and IP_3 receptor antagonist, 2-APB, on NAADP-induced acrosome reaction. To evaluate the functional relation between NAADP-triggered acrosomal secretion and intracellular Ca^{2+} channels, permeabilized sperm were pre-treated for 15 min at 37 °C with 10 µM ruthenium red ([**B**], [*RR*]) or 10 µM 2-APB ([**C**], [*2-ABP*]), followed by a stimulation with the indicated concentrations of NAADP (30 min). Note that significant inhibition of acrosomal exocytosis by RR was registered only at 50 µM NAADP. In contrast, 2-ABP significantly attenuated acrosome reaction upon application of all three NAADP doses. The results are presented as mean values of 6 - 10 independent experiments ± SEM of acrosomal exocytosis index. Statistical significance (paired Student`s t-test) [*: $p < 0.05$], [**: $p < 0.01$], [***: $p < 0.001$] was calculated comparing samples incubated with one of the three NAADP doses to corresponding probes pretreated with inhibitors.

Figure S6. TPC1 associates with Triton X-100-resistant membrane microdomains isolated from rat spermatozoa.
Rat sperm membranes (P_{100}) were extracted with 1.5 % Triton X-100 for 30 min at 4 °C. Subsequently, lysates were separated by centrifugation (2 h, 50,000g), thus yielding in a detergent-soluble (S_{TX}) and Triton X-100 insoluble membrane fraction (P_{TX}). Following protein determination, equal amounts of protein from each fraction were subjected to Western blot analysis for TPC1 (top panel), IP_3-R (middle panel) and caveolin-1 (bottom panel). Note that the bulk of TPC1 and IP_3-R co-migrated with caveolin-1 in the Triton X-100 insoluble pellet (P_{TX}). Representative Western blots of three experiments from two independent rat tissue preparations are shown.

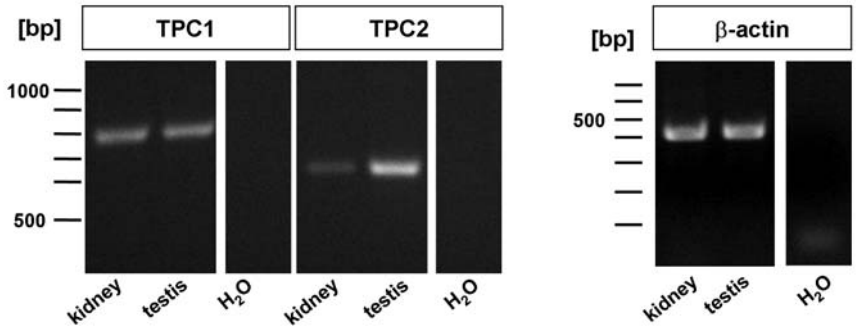

Suppl. Figure S1
Arndt et al.

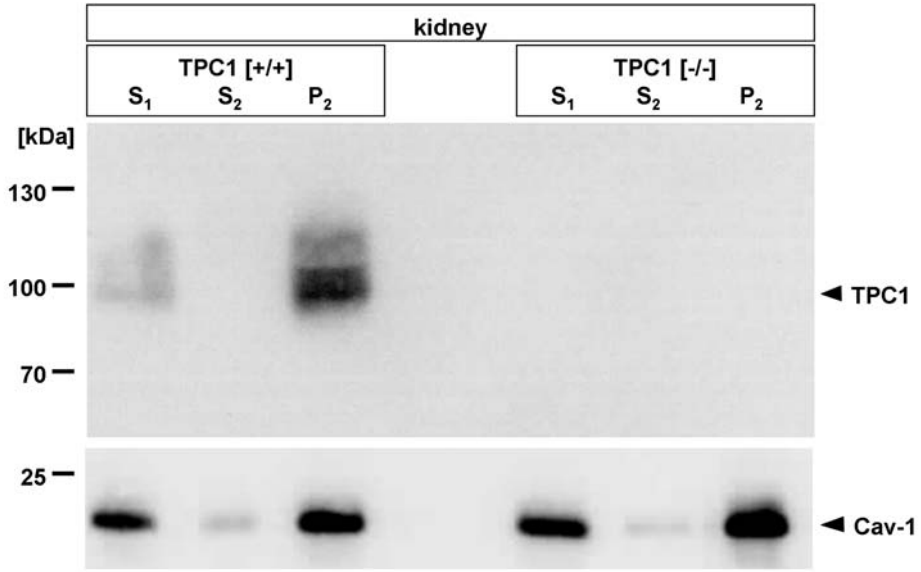

Suppl. Figure S2
Arndt et al

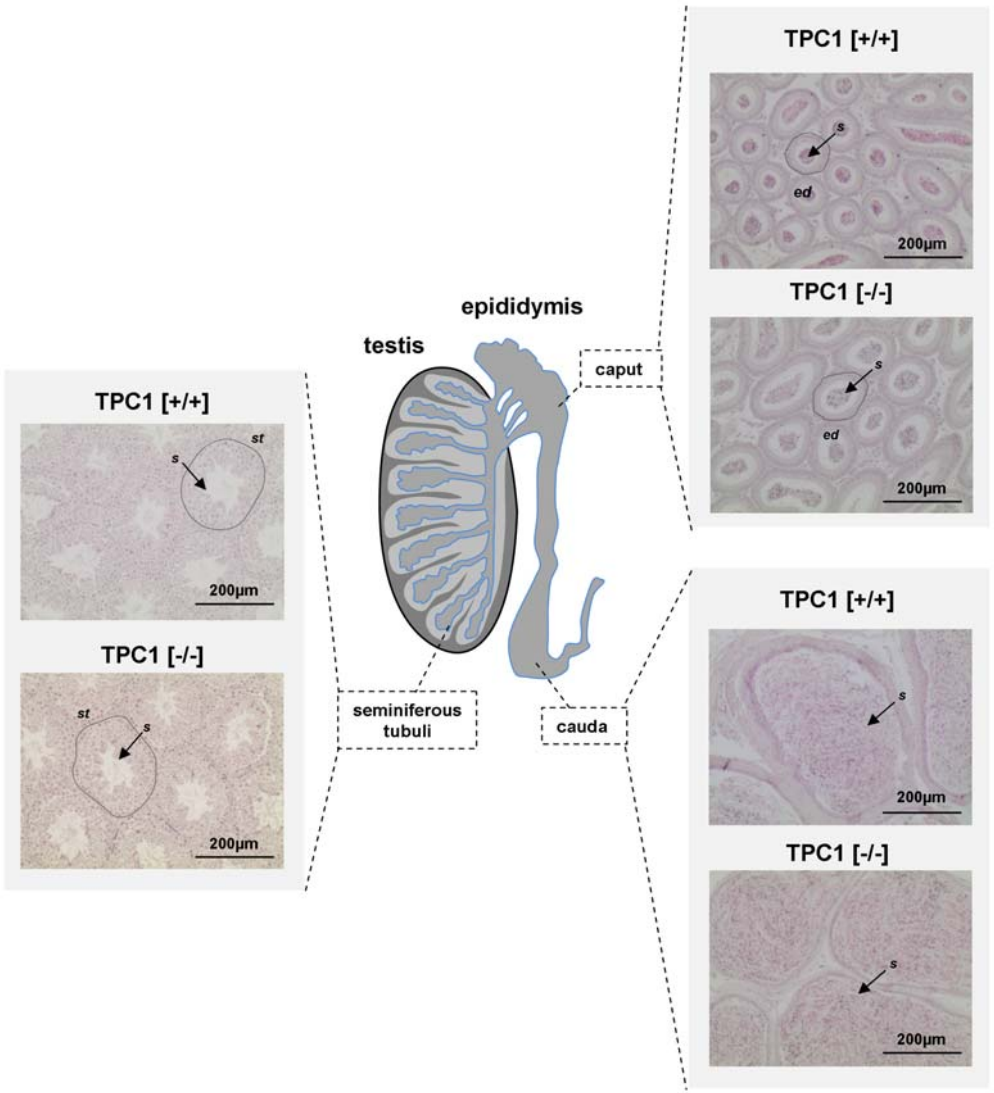

Suppl. Figure S3A
Arndt et al

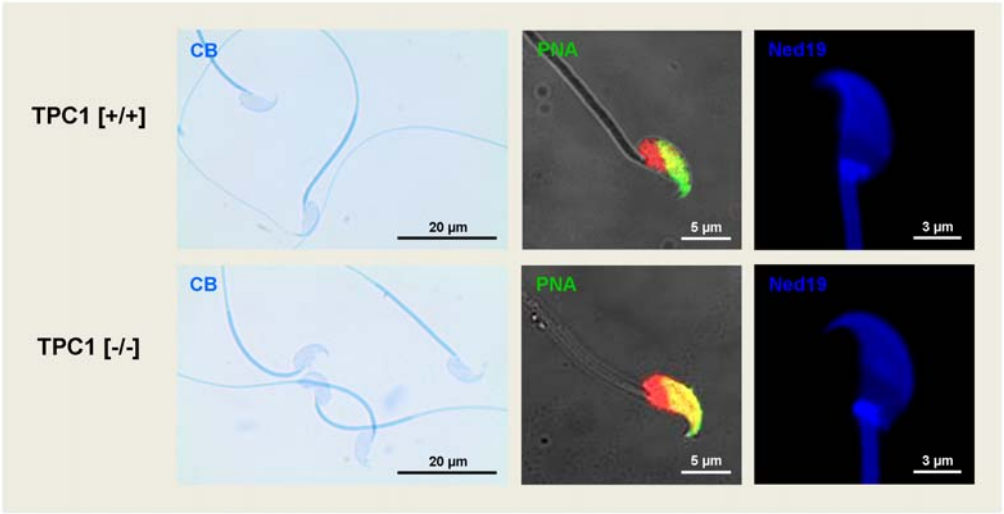

Suppl. Figure S3B
Arndt et al

A

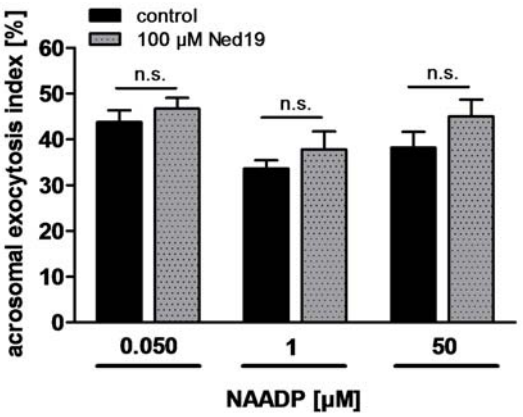

B

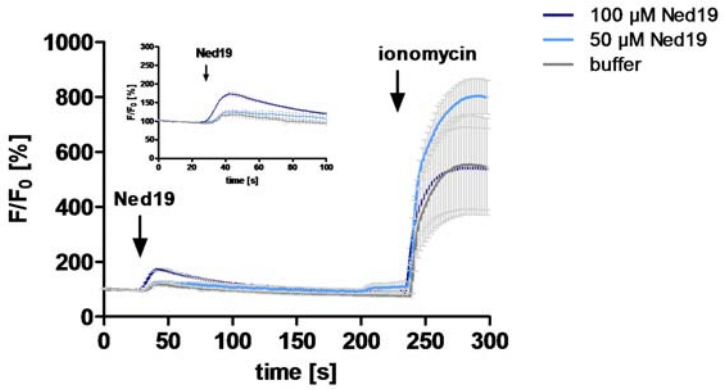

Suppl. Figure S4
Arndt et al

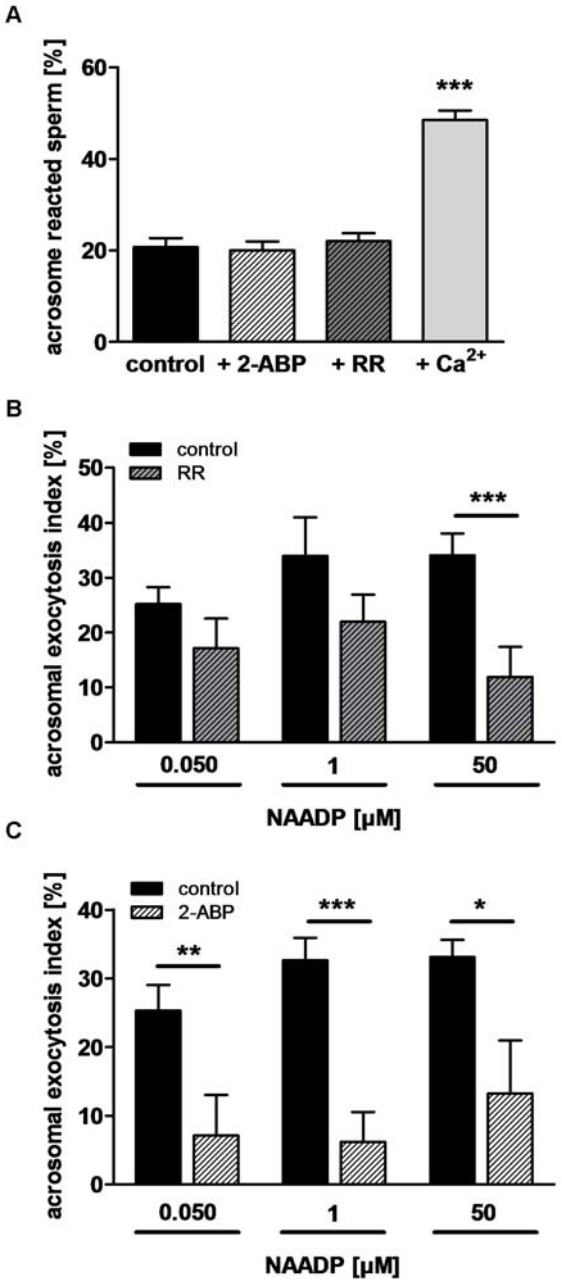

Suppl. Figure S5
Arndt et al

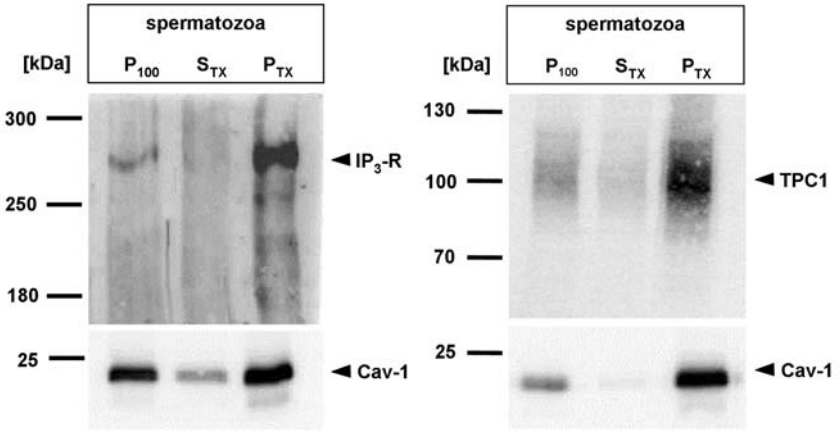

Suppl. Figure S6
Arndt et al